MEASURED AND CALCULATED FIELD PROPERTIES OF THE SIS 100 MAGNETS DESCRIBED USING ELLIPTIC AND TOROIDAL MULTIPOLES

E. Fischer†, P. Schnizer, A. Mierau GSI, Darmstadt, Germany
P. Akishin, JINR, Dubna, Russia
R. Kurnyshov, Elektroplant, Moscow, Russia
B. Schnizer, TUG, Graz, Austria
P. Shcherbakov, IHEP, Protvino, Russia

Abstract

The first full size superconducting dipole magnets for the SIS 100 Tm synchrotron were built and tested. The achieved magnetic field has been measured with a rotating coil probe.

An intensive Finite Element R&D, necessitated by the used superconducting cable as well as by the complex mechanical coil and yoke structure, allows calculating the field with high accuracy.

Elliptic multipoles were used to describe the field within the whole aperture of the vacuum chamber. As the final design for the SIS 100 dipoles is curved, we developed toroidal multipoles describing the field within a curved magnet, and enabling us to interpret the measurement of a rotating coil probe within such magnets.

We describe the performance of the magnetic measurement system, present the measured field properties and compare them to the calculated ones.

INTRODUCTION

The SIS 100 synchrotron, the core component of the Facility for Antiproton and Ion Research, will be the world's second machine using fast ramped superconducting magnets. The magnets use a Nuclotron cable (i.e. a hollow tube cooled by forced two phase helium flow with superconducting wires wrapped around this tube). The magnetic field quality is dominated by the iron field. During the R&D phase we have been developing the theory to describe the magnetic field within elliptic apertures [1, 2] as well as for curved magnets [3] next to test calculations and studies on FEM codes [4] as well as building a magnetic measurement system [5] for such magnets. First full size prototype magnets have been built and the first one already tested [6]. In this paper we compare the calculated field quality next to the measured one.

* This work is supported by the EU FP6 Design Study (contract 515873 - DIRAC secondary beams)

† e.fischer@gsi.de

THEORY

Elliptic Multipoles

The field within the elliptic beam aperture is described using elliptic multipoles for elliptic coordinates of the type $x = e\cosh\eta\cos\psi$, $y = e\sinh\eta\sin\psi$ with x and y the Cartesian coordinates and η and ψ the elliptic coordinates with $0 \le \eta \le \eta_0 < \infty$ and $-\pi \le \psi \le \pi$. The field $\mathbf{B} := B_y + iB_x$ can be described within the whole ellipse using

$$\mathbf{B}(\eta,\psi) = \sum_{q=0}^{M} \mathbf{E}_q \, \cosh[q(\eta + i\psi)]/\cosh(q\eta_0), \quad (1)$$

with $\eta_0 = \tanh^{-1}(b/a)$ the reference ellipse and a and b its half axes [1, 2] (here $a = 45\,mm$ and $b = 17\,mm$). These $\mathbf{E}_q$ can be recalculated to circular multipoles

$$\mathbf{B}(\mathbf{z}) = \mathbf{B}_m \sum_{n=1}^{M} \mathbf{c}_n \, (\mathbf{z}/R_0)^{n-1} \quad (2)$$

using an analytic linear transformation, with $\mathbf{B_m}$ the main field, $\mathbf{z} = x + i\,y$, R_0 the reference radius and $\mathbf{c}_n = b_n + i\,a_n$ the relative higher order circular multipoles. The b_n's and a_n's are dimensionless constants. In this paper they are given in units i.e. $1\,unit = 100\,ppm$ at a R_0 of $40\,mm$. Using (2) the field can be interpolated with sufficient accuracy within an ellipse with half axes a, b.

Toroidal Multipoles

In the gap of a curved magnet a torus segment ($-\varphi_0 \le \varphi \le \varphi_0$) is used as reference volume. Dimensionless local toroidal coordinates ρ, ϑ, φ are defined by

$$X + iY = R_c\,h\,e^{i\varphi},\ \ Z = R_{Ref}\sin\vartheta,\ \ h = 1 + \epsilon\rho\cos\vartheta,$$

with R_{Ref} (R_c) the minor (major) radii of the torus and $\epsilon := R_{Ref}/R_c < 1$ the inverse aspect ratio describing the magnitude of the curvature effects. The centre of the fundamental Cartesian system (X, Y, Z) coincides with that of the torus, Z is normal to the equatorial plane. The quasi-radius $\rho \cdot R_{Ref}$, $0 \le \rho \le 1$, is the normal distance of the field point from the centre circle $Z = 0$, $\sqrt{X^2 + Y^2} = R_c$; the poloidal angle $-\pi \le \vartheta \le \pi$, is around the centre circle;

the toroidal angle $-\pi \leq \varphi \leq \pi$ agrees with the common azimuth. Only toroidally uniform fields are considered; their field components B_x, B_y are confined to the planes φ = const. and are independent of φ. (x, y) are local Cartesian coordinates in these planes; the $x-$, $(y-)$ axes are parallel to the $X-, (Z-)$ axes. The potential equation for toroidally uniform fields is (neglecting a constant factor)

$$\left[\frac{\partial^2}{\partial\rho^2} + \frac{1}{\rho}\frac{\partial}{\partial\rho} + \frac{1}{\rho^2}\frac{\partial^2}{\partial\vartheta^2} + \frac{\epsilon}{h}\left(\cos\vartheta\,\frac{\partial\Phi}{\partial\rho} - \frac{\sin\vartheta}{\rho}\,\frac{\partial\Phi}{\partial\vartheta}\right)\right]\Phi$$
$$= h^{-1/2}\left[\frac{\partial^2}{\partial\rho^2} + \frac{1}{\rho}\frac{\partial}{\partial\rho} + \frac{1}{\rho^2}\frac{\partial^2}{\partial\vartheta^2} + \frac{\epsilon^2}{h^2}\right]\left(h^{1/2}\,\Phi\right) = 0, \quad (3)$$

with the terms in the square brackets the Laplacian in plane polar coordinates ρ, ϑ. The last term, due to the curvature, introduces contributions which may be represented as a power series in the inverse aspect ratio ϵ. Approximate toroidal multipoles accurate to order ϵ can be obtained by (see second line):

$$\Phi_m(\rho,\vartheta) = h^{-1/2}\,\rho^{|m|}\,e^{im\vartheta} + O(\epsilon^2), \quad (4)$$
$$\approx \rho^{|m|}\,e^{im\vartheta} - \frac{\epsilon}{4}\,\rho^{|m|+1}\left(e^{i(m+1)\vartheta} + e^{i(m-1)\vartheta}\right).$$

$$\bar{\Phi}_m(x,y) \approx \mathbf{zs}^{|m|} - \frac{\epsilon}{4}\left[\mathbf{zs}^{|m|+1} + \mathbf{zs}^2\,\mathbf{zs}^{|m|-1}\right]. \quad (5)$$

with $\mathbf{zs} = \mathbf{z}/R_0 = x + iy/R_0 = \rho\, e^{i\vartheta}$. The multipoles are orthogonal w.r.t. the scalar product

$$(\Phi_m, \Phi_k) := \int_{-\pi}^{\pi} \Phi_m^*(\rho,\vartheta)\Phi_k(\rho,\vartheta)\, h\, d\vartheta = [\rho^{|m|}]^2\, 2\pi\, \delta_{mk}.$$

The expansion coefficients τ_m of a given potential

$$\Phi(\rho,\vartheta) = \sum_{m=-\infty}^{\infty} \tau_m\, \Phi_m(\rho,\vartheta) \quad (6)$$

are defined by the values given along the reference circle $\rho = 1$:

$$\tau_m = \frac{1}{2\pi}\left(\Phi_m(1,\vartheta), \Phi(1,\vartheta)\right) \quad (7)$$

This theory can be expanded to vector fields (required e.g. to interpret rotating coil measurements in a curved magnet) [7].

MAGNETIC FIELD

Measurement method

The magnetic field was measured with a "Mole", i.e. a rotating coil probe system with all auxiliary equipment working in the magnetic field [5]. The rotating coil probe is equipped with dipole compensation windings and thus allows to measure the magnetic field homogeneity with a higher accuracy than the main field. The field was now measured at different lateral positions ($x = \pm 3, 0\,cm.$) (see Fig. 2). The higher accuracy of the field homogeneity measurement allows correcting the relative measurement error of $\mathbf{C_1^{l,r}}$ minimising the offset between both measurements

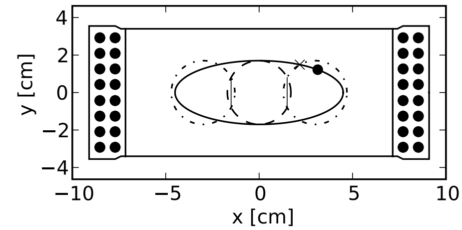

Figure 2: The gap of the measured magnet as well as the measurement positions of the coil probe. black filled circles — coil windings, dashed centre circle, dashed dotted circle x_m = ± 3.0 cm, coil probe measurement positions, solid line — ellipse used in reconstruction, dot on the ellipse – angle ψ_c, solid vertical lines – minimization lines.

along the overlap (vertical lines Fig. 2) using the adjustment function

$$\mathbf{C_m} = (1 + g/10000)\,\bar{\mathbf{C}}_\mathbf{m}\,\exp(im\beta) \quad (8)$$

with g correcting the integrator gain or the longitudinal coil positioning precision (end field measurements) and β the field direction uncertainty. g was typically 5 for the central field, 20 for the end field, β typically below 1 mrad and thus the adjustments fit well with measurement precision of the used system. The data on the ellipse (a = 4.5 cm, b = 1.7 cm) were reconstructed using

$$\mathbf{B_i}(\mathbf{z}) = \lambda\sum_{m=0}^{M_m}\mathbf{C_m^c}\left(\frac{\mathbf{z}}{R_m}\right)^{m-1} + (1-\lambda)\sum_{m=0}^{M_m}\mathbf{C_m^{l,r}}\left(\frac{\mathbf{z}-x_m}{R_m}\right)^{m-1}$$

with M_m = 10 and defining λ by

$$\lambda(p_0) = 0 \quad \lambda(p_1) = 1 \quad \lambda'(p_0,p_1) = 0 \quad \lambda(p) = 3p^2 - 2p^3$$

with

$$p = \begin{cases} 0 & \psi' < p_0 \\ \frac{2\psi'-\pi}{2p_0-\pi} & p_0 \leq \psi' \leq \pi. \end{cases}$$

with $\psi' = \psi$ for the first $\pi - \psi$ for the second, $\psi - \pi$ for the third and $\psi - 2\pi$ for the forth quadrant [1, 2]. λ models the weight of each measurement with respect to the other with the free parameter ψ_c, which is chosen such that $\lambda(p(\psi))$ reassembles the weight (i.e. the inverse accuracy) of each measurement assuming that its given by $R_m/(\mathbf{z} - x_0)$ [2]. Based on the field reconstructed on the ellipse, elliptic multipoles eq. (1) and, using the transformation matrix [1, 2], circular multipoles eq. (2) were calculated.

DC field

The static field was calculated using TOSCA in 3D [8] and using ANSYS in the central region of the magnet [9]. The calculated and measured transfer function $t_f = B_0/I$ with I the current is given in Fig. 1(a).

One can see that the calculated is slightly higher than the measured one. Further the iron non linearity at low fields

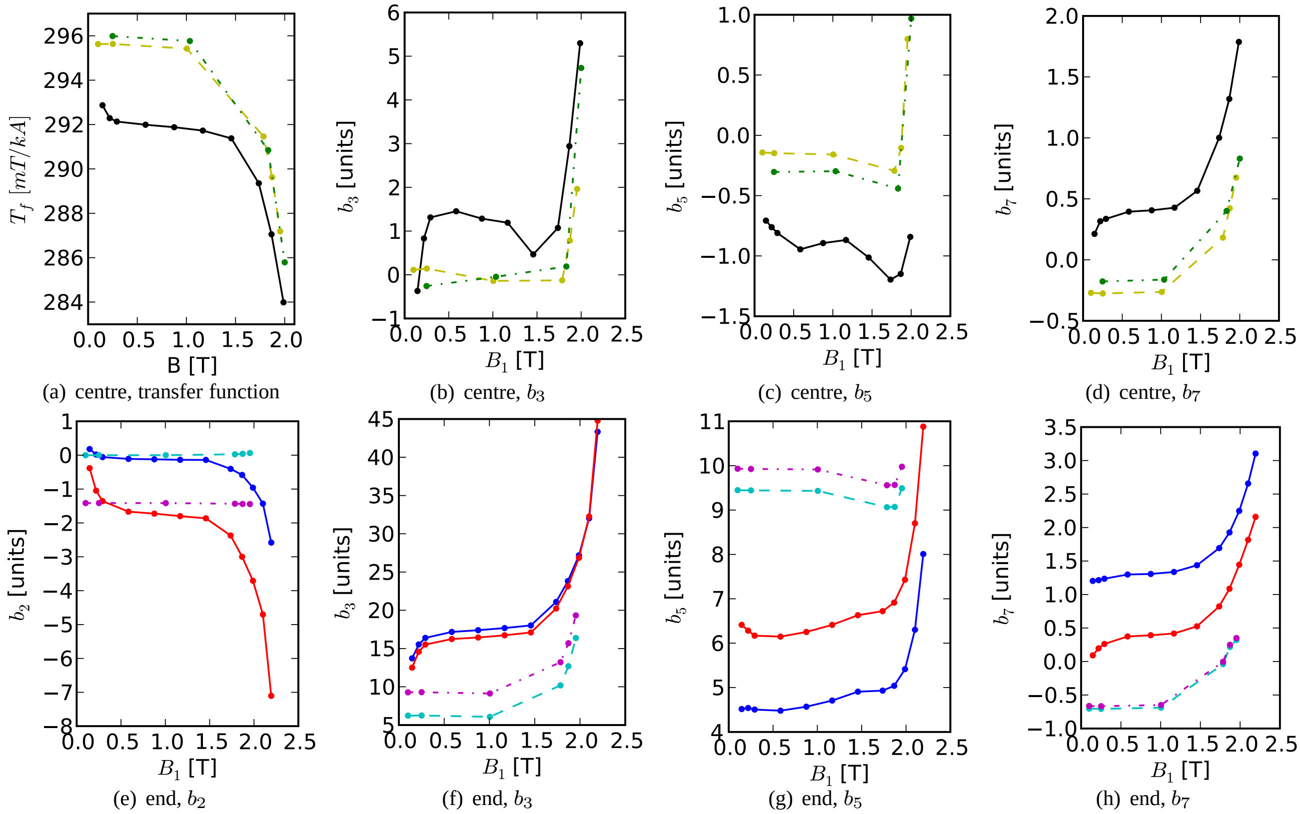

Figure 1: The measured (solid line) and calculated transfer function and harmonics versus the main field. centre: black – measured, yellow – TOSCA, green – ANSYS. end: connection side blue – measured, cyan – TOSCA; non connection side: red – measured, mangenta – TOSCA.

is not reproduced. For the central field the calculated saturation effect is nicely reproduced for b_3 and b_7 but not for b_5 (see Fig. 1(b) - 1(d)). For the end field, measured with the centre of the 60 cm long coil probe at $z = \pm 120\,cm$, one can see that the measured multipoles have a similar shape as the calculated ones but with a constant offset (see Fig. 1(f) - 1(h)). b_3 shows a deviation at low field similar to the deviation of the transfer function at low field.

CONCLUSION

The first SIS 100 full size dipole magnet has been built, and its field quality calculated as well as measured. The calculated transfer function, using catalog data for room temperature, is $\approx 1\,\%$ higher than the measured one as well as the calculated data do not show the nonlinearity at injection. The higher order multipoles were given for the central field next to the end field. The curves agree quite well in shape but have an offset as well as different behaviour at low field where the permeability curve does not take the remanence into account. Still the calculated results are of good quality and agree well with the measurements. Using a bigger coil probe as well as readjusting the hysteresis curve using the measured data we are confident to further increase the quality of the prediction.

REFERENCES

[1] P. Schnizer, B. Schnizer, P. Akishin, and E. Fischer. “Theoretical field analysis for superferric accelerator magnets” EPAC’08, Genova, July 2008

[2] P. Schnizer, B. Schnizer, P. Akishin, and E. Fischer. “Plane elliptic multipole representations of static magnetic fields”, Submitted to NIMA, 2008.

[3] P. Schnizer, B. Schnizer, P. Akishin, and E. Fischer. “Plane elliptic or toroidal multipole expansions”, IGTE, September 2008, Graz

[4] E. Fischer, R. Kurnishov, and P. Shcherbakov, Cryogenics, 47:583–594, 2007.

[5] P. Schnizer et al, “Mole for measuring pulsed superconducting magnets” IEEE Trans. Appl. Supercon. p.1648–1651 18 (2008)

[6] E. Fischer et al, “Fast Ramped Superferric Prototype Magnets of the FAIR Project”, this conference

[7] P. Schnizer, B. Schnizer, P. Akishin, and E. Fischer, “Plane elliptic or toroidal multipole expansions”, COMPEL, 28(4), 2009.

[8] P. Schnizer et al, “Superferric magnets for the SIS 100 synchrotron”, IGTE, September 2008, Graz

[9] E. Fischer et al, “ Numerical analysis of the operation parameters of fast cycling superconducting magnets”, ASC08, August 2008, Chicago